SAND78-0625
Unlimited Release
UC-62

Performance Testing of the McDonnell Douglas Fresnel Lens Solar Collector

Vernon E. Dudley, EG&G, Inc.
Robert M. Workhoven

Prepared by Sandia Laboratories, Albuquerque, New Mexico 87185 and Livermore, California 94550 for the United States Department of Energy under Contract AT(29–1)-789

Printed February 1979

Sandia Laboratories

SF 2900 QD (4-78)

Issued by Sandia Laboratories, operated for the United States Department of Energy by Sandia Corporation.

Printed in the United States of America

Available from
National Technical Information Service
U. S. Department of Commerce
5285 Port Royal Road
Springfield, VA 22161

Price: Printed Copy **$4.50** ; Microfiche $3.00

SAND78-0625

PERFORMANCE TESTING OF THE McDONNELL DOUGLAS FRESNEL LENS SOLAR COLLECTOR

Vernon E. Dudley
EG&G, Inc.

Robert M. Workhoven
Experimental Systems Operations Division 4721
Sandia Laboratories
Albuquerque, NM 87185

ABSTRACT

This report summarizes the results of tests performed on the McDonnell Douglas Fresnel Lens rotating array solar collector at the Midtemperature Solar Systems Test Facility. Test objectives are defined, test procedures are described, and test results and conclusions are given.

CONTENTS

ILLUSTRATIONS

TABLES

PERFORMANCE TESTING OF THE
McDONNELL DOUGLAS FRESNEL LENS SOLAR COLLECTOR

INTRODUCTION: A series of solar collector designs are being tested in Sandia Laboratories' Collector Module Test Facility (CMTF) as a part of the Department of Energy's continuing program to characterize selected collector modules for possible future system use (Reference 1). Several of the collector designs that are being tested have been chosen to provide the energy input for large demonstration projects throughout the nation. The McDonnell Douglas design, which is designated as a Linear Fresnel Lens Rotating Array Solar Collector, utilizes several lenses in a rectangular aluminum housing that tracks the sun by azimuth and elevation angle movements. A photograph of the collector is shown in Figure 1.

TEST OBJECTIVE: The objective of this test series was to characterize the performance of the Linear Fresnel Lens Rotating Array Solar Collector designed by McDonnell Douglas Aerospace Corporation of Huntington Beach, California. Items of particular interest were the peak thermal efficiency, the all-day efficiency and the receiver thermal losses at fluid temperatures from 100-300^{o}C.

COLLECTOR DESCRIPTION: A sketch of the Linear Fresnel Lens Rotating Array Solar Collector is shown in Figure 2. The collector is ≈3.63 m by 5.94 m by 1.07 m deep. The ends are tapered, resulting in an ≈4.75 m length at the lens whereas the bottom is ≈5.94 m long. This housing and the internal frames are constructed of aluminum. The housing is mounted on a pedestal which places the bottom of the housing ≈1.5 m above the ground. The collector rotates about the pedestal, resulting in azimuth motion, and rotates about hinge points to change the elevation

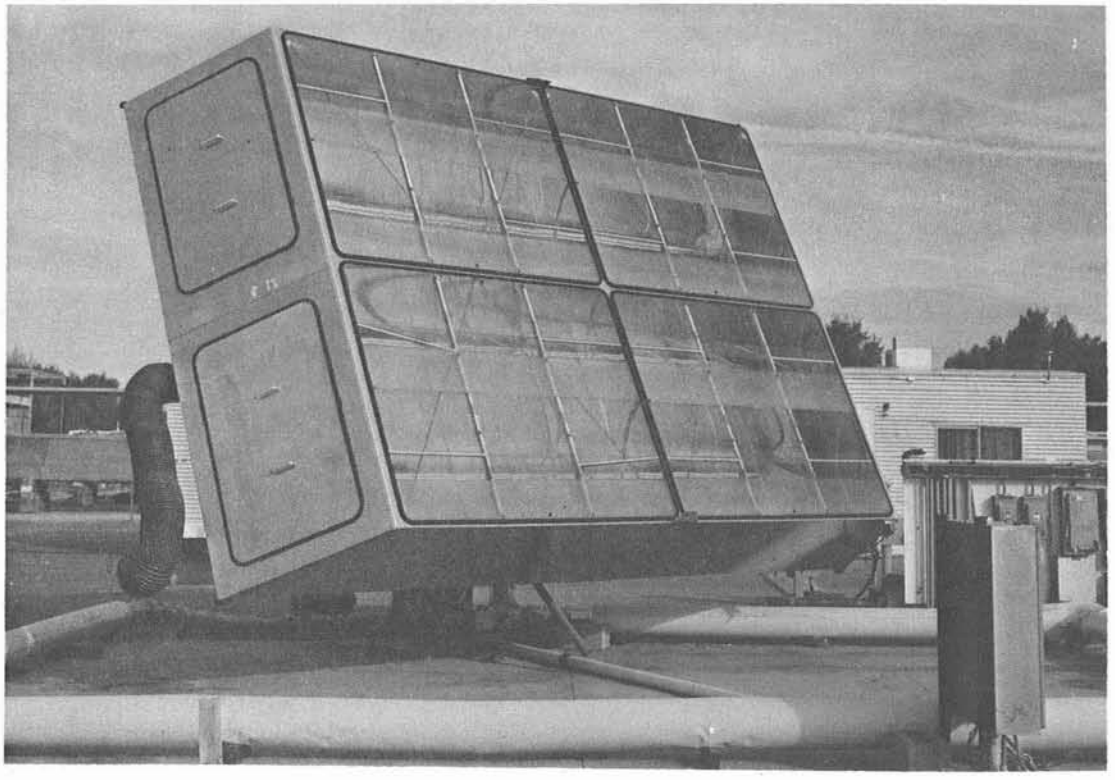

Figure 1. McDonnell Douglas Linear Fresnel Lens Rotating Array Solar Collector.

angle to provide two-axis tracking during the day. The azimuth motion is obtained with an orbidrive, which is a drive train providing a large gear reduction. The elevation angle is positioned by a screw-jack linear actuator. Both positioning mechanisms are driven by 240-V, three-phase, electric motors.

The tracking motors are actuated by a tracking controller. This controller monitors the output signals from a solar sensor unit to provide closed-loop tracking of the sun. Initial acquisition of the sun in this test unit is accomplished manually using dials on the tracking controllers. The solar sensor is mounted on the collector housing.

The cast-acrylic lenses are the linear Fresnel type with an F number of 1.0, and were manufactured by Swedlow, Inc. The focal length of the lens is ≈0.93 m. The lens aperture for each of the four absorber tubes is 3.89 m^2. The total lens aperture for this unit is 15.56 m^2.

The receiver system that is sketched in Figure 3 includes an absorber tube, an absorber tube plug, reflectors, glazing, and insulation. Both the absorber tube and plug are low carbon steel. The absorber tube is 3.81 cm O.D. with an outer surface plating of black chrome to improve the surface optical characteristics. A plug is placed in the absorber tube to decrease the cross-sectional flow area. This plug consists of 2.222 cm O.D. tubing with the ends plugged. The glazing is a low iron glass manufactured by ASG Industries, Inc., and has the trade name Lustraglass. The insulation is layers of glass fiber batts encased in a glass cloth. Both the insulation and the glazing are included in the system to reduce the thermal loss from the receiver. The reflectors are stainless steel and aid in capturing stray solar rays which have not been focused on the tube. There are four receivers in this collector and a 2.54-cm-diameter, insulated, cross-over tube connects the ends such that all four of the tubes are in series in the flow loop.

The size of the McDonnell Douglas Collector (15.56 m^2) tested at the CMTF was a compromise that minimized fabrication costs, but still produced a reasonably large collector that would provide credible test results. McDonnell Douglas has the opinion that, in a large solar installation, collectors up to 90 m^2 in size could be deployed on a single pedestal to provide optimum economy.

TEST FACILITY DESCRIPTION: The CMTF's fluid loop 1 is designed to supply Therminol 66 as a heat-transfer fluid at temperatures from about 100-300°C. Characteristics of Therminol 66 are given in Reference 2. The design flow-rates that are available in Loop 1 range from 4 L/min to 40 L/min. Details concerning this fluid loop test facility can be found in Reference 3.

A typical test day began by heating the fluid loop with electric heaters to the desired collector input temperature. Data collection was usually attempted at only one temperature in one day due to the time required for temperature stabilization. During an individual test, both the input temperature and the flow-rate were maintained constant while the output temperature varied according to the test conditions.

Seven platinum resistance temperature sensors were used to measure fluid temperatures. These sensors measured the temperatures at each end of two of the four absorber tubes and at input and output of the total collector array. Temperature sensor electronics calibration was checked at frequent intervals throughout the test series.

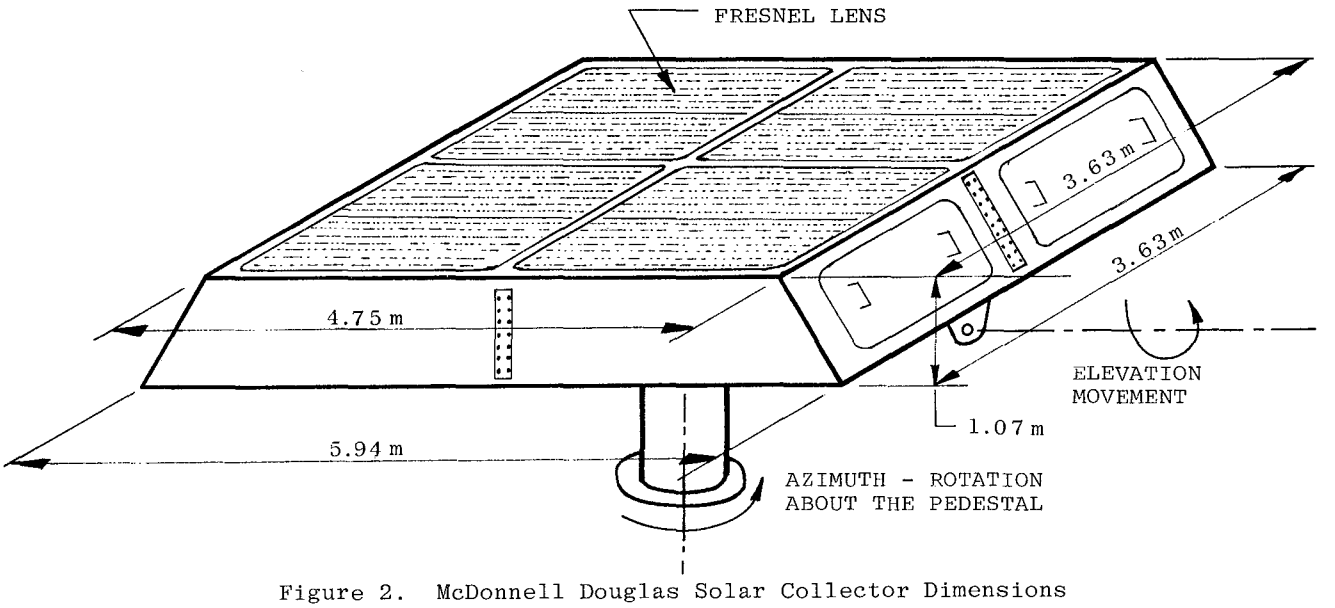

Figure 2. McDonnell Douglas Solar Collector Dimensions

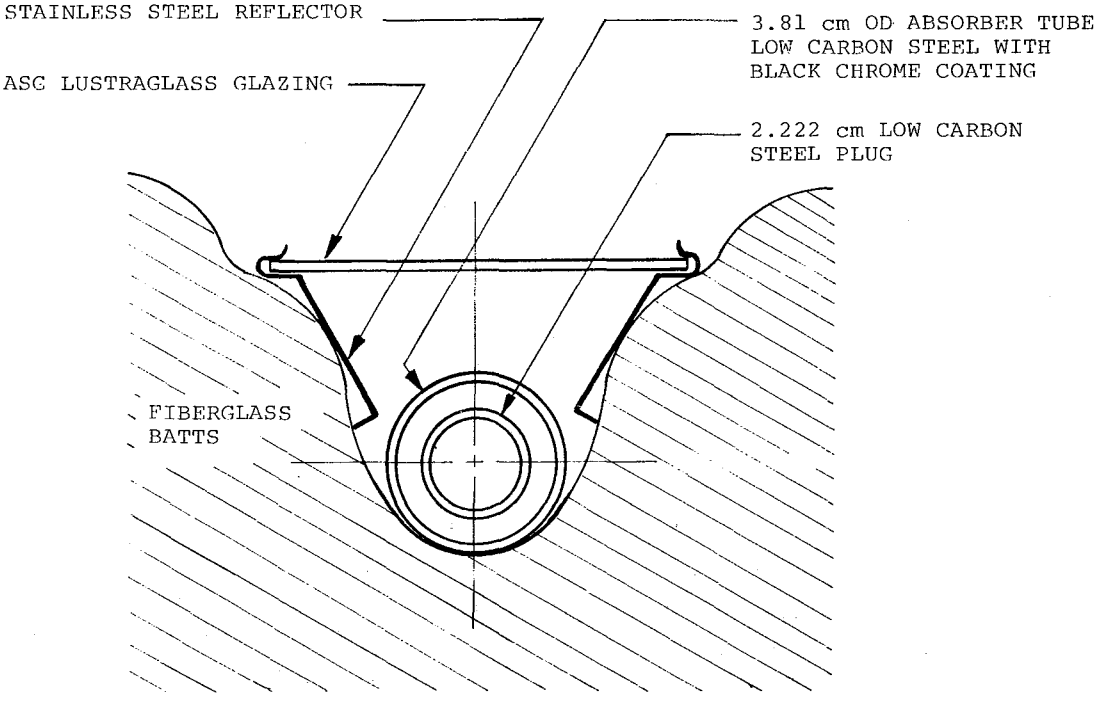

Figure 3. McDonnell Douglas Receiver Assembly

Fluid flow-rate was measured with a turbine flowmeter manufactured by Flow Technology, Inc. Prior to the test series, the flowmeter was calibrated by flowing fluid into a container. The fluid container weight vs. time was measured to determine the true flow-rate.

Direct solar radiation measurement was provided by an Eppley pyrheliometer. Ambient temperature, wind speed and wind direction were also recorded.

The data from the instruments described above were converted to digital format by Doric 210 and 220 analog-to-digital data systems. An HP 2116 minicomputer processed the input data and a printed sheet of the critical data for the test being performed was provided as output.

Figures 4 and 5 contain reproductions of the printed output for an efficiency test and for a thermal loss test, respectively. In Figures 4 and 5 the temperatures listed are in degrees Celsius. The delta temperature that is listed in Figures 4 and 5 is the arithmetic difference of the input and output temperatures.

The speed of the data system was such that all of the data channels could be read, the calculations could be performed, and a line in the data table printed in about 40 seconds. Seventy-seven measured and calculated data values from the data system were recorded on magnetic tape every 40 seconds. Only those shown in Figures 4 or 5 were printed in real time. The average values were automatically printed after ten data points were accumulated. The complete data printout (as shown in Figures 4 and 5) was repeated at intervals of about 7 minutes throughout a test run. The number of decimal places printed in Figures 4 and 5 should not be taken as indicating the data system accuracy since the choice of the print format was dictated by the peculiarities of the computer system. Either a loss or an efficiency data print was made continuously when the system was operating; however, only those data blocks occurring under stable conditions are included in this report.

PERFORMANCE TEST DEFINITIONS: During a test run both the specific heat and density of the Therminol 66 were calculated for each data set using the average temperature of the fluid in the absorber tube and the properties of Therminol 66 (furnished by the Monsanto Industrial Chemicals Company, Reference 2). Heat gain (or loss) was then calculated by using the following formula:

$$Q = m\, C_p\, \Delta T$$

in which

Q = heat gain, kJ/hr

m = mass flow-rate of fluid, kg/hr

C_p = specific heat of fluid, J/kg^{o}C

ΔT = in-out temperature differential, ^{o}C

A successful loss measurement is defined as one in which the values for input and output temperatures remained constant to within 0.1^{o}C or less, the flow-rate varied by 0.1 L/min or less and the delta temperature changed by 0.1^{o}C or less. Most of the loss test data points reported are averages of four to six data blocks with conditions nearly constant over the entire time averaged. A data block contained ten measurement points. Loss tests were conducted with the lens system defocused

MDAC COLLECTOR EFFICIENCY TEST

JULIAN DAY 317 HOUR 12 MINUTE 38 SOLAR TIME

14.4 (DEG C) AMBIENT TEMPERATURE (DEG F) 58
9 WIND DIRECTION: DEGREES
1 WIND SPEED: MPH

SKIN TEMPS	537.8	275.2	153.7	255.8	284.5

TEMP IN	TEMP OUT	SOLAR W/M^2	DELTA TEMP	FLOW L/MIN	EFFICIENCY PERCENT
252	264.61	983.7	12.6	16.1	39.6
252	264.61	983.9	12.6	16.1	39.8
252	264.61	983.4	12.6	16.1	39.7
252	264.61	983.7	12.6	16.1	39.7
252	264.56	981.4	12.6	16.1	39.7
252.06	264.56	981.4	12.5	16.1	39.6
252.06	264.56	980.5	12.5	16.1	39.5
252	264.56	980.4	12.6	16.1	39.6
252	264.56	982.2	12.6	16.1	39.7
251.94	264.56	983.3	12.6	16.1	39.9
		10 POINT AVERAGES			
252.006	264.58	982.39	12.5722	16.0883	39.6896

Figure 4. Typical Data Printout From Efficiency Test.

MDAC THERMAL LOSS TEST

JULIAN DAY 326 HOUR 14 MINUTE 59 SOLAR TIME

15.2 (DEG C) AMBIENT TEMPERATURE (DEG F) 59.3
307 WIND DIRECTION: DEGREES
-4 WIND SPEED: MPH

SKIN TEMPS	537.772	227.889	119.889	229.5	225.778

TEMP IN	TEMP OUT	FLOW L/MIN	DELTA TEMP	WATTS GAIN/LOSS
229.17	227.44	38.8	-1.72	-1503.2
229.17	227.44	38.9	-1.72	-1485.5
229.17	227.5	38.8	-1.67	-1461.6
229.17	227.5	38.8	-1.67	-1462.7
229.17	227.5	38.9	-1.67	-1464.3
229.17	227.44	38.8	-1.72	-1461.5
229.17	227.44	38.8	-1.72	-1473
229.22	227.44	38.9	-1.78	-1519.2
229.22	227.5	38.9	-1.72	-1495.2
229.22	227.5	38.8	-1.72	-1483.5
		10 POINT AVERAGES		
229.183	227.472	38.8482	-1.71116	-1480.97

Figure 5. Typical Data Printout From Thermal Loss Test.

so that the light was focused on the floor of the collector box. No light from the lenses struck any part of the receiver tube assembly. Thermal losses were measured on sunny days in conjunction with efficiency tests since cloudy-day thermal losses are not representative of operating conditions.

For an efficiency test, efficiency was calculated from the following formula:

$$\eta = \frac{Q/A}{I}$$

in which

η = solar collector efficiency

Q = heat gain, W

A = collector aperture area, m^2

I = direct solar radiation, W/m^2

An efficiency measurement at a single temperature and flow-rate was made for a period long enough to assure complete temperature and flow stabilization. The all-day efficiency test was run at a constant flow-rate and input temperature without interruption for the entire day in order to define the efficiency of the concentrator at various levels of solar radiation. This test began as early as operating temperatures could be established and continued for four hours past solar noon.

A successful efficiency measurement is defined as one in which at least one of the ten-point data blocks had input and output temperature changes of $0.1^{o}C$ or less, flow-rate variations of 0.1 L/min or less, the delta temperature remained within $0.1^{o}C$ or less and solar radiation remained constant to about 1%. Temperatures, flow-rate and insolation had to be as nearly as stable as described above for at least five to ten minutes prior to the measured data point to be acceptable. Efficiency measurements are normally made with insolation greater than about $900\ W/m^2$.

The temperature, flow-rate and insolation stability criteria outlined above are necessary because the heat gain formula given assumes steady-state conditions. If near steady-state conditions can be achieved during a collector test, the computed values for heat gain (or loss) and efficiency will be nearly constant also, with some scatter in the data due to noise. Because of the thermal mass of the collector system, any change in temperature, flow-rate or insolation will result in measurements that do not correctly represent the performance of the collector.

Even on a sunny day that appears ideal for testing a solar collector, there are still variations in solar radiation. However, these variations can be relatively small, as can be seen in several of the test data plots later in this report. Small, rapid variations of this kind produce scatter in the efficiency data, but no long-term systematic errors.

As operated at the CMTF, the heat-transfer fluid supply loop tends to produce fluid flow-rate variations similar to those seen in the solar radiation input: Small, rapid fluctuations with no long-term trend towards a higher or lower rate. These variations also produce scatter in the measured data.

Small rapid temperature fluctuations also appear in the measured data, again producing data scatter. However, the temperature measurements are subject to fairly long-term, slow changes which can result in fairly large, systematic errors in heat

gain/loss and efficiency calculations. One typical source of this kind of temperature drift is the constantly increasing temperature that occurs each test day as the system is heated towards the intended operating temperature. Another is the temperature decay that continues for very long times after the collector system is defocused to begin a thermal loss test.

At the CMTF, collector input and output temperatures are usually measured less than one second apart in time. However, the fluid whose temperature is being measured at the collector input may not arrive at the collector output for a relatively long time--from several seconds up to several minutes. Thus an efficiency, or heat gain/loss, measurement will not be valid unless the input and output temperatures are stable for at least as long as the transit time of the heat-transfer fluid through the system.

Because of the thermal mass of both the fluid supply system and the collector, stable temperatures must be held for relatively long periods of time before the complete system is in thermal equilibrium and valid measurements can be made. A small constant drift in temperatures can produce test data that looks quite acceptable; however, it contains a systematic error because of the thermal mass shift of in/out delta temperature. An example is shown later in this report (Figure 11) where a constant temperature increase of $0.7^{\circ}C$ per minute produces an efficiency measurement that has a very small data scatter and has a nearly constant efficiency value for more than an hour. This measured efficiency value turns out to be 5 percentage points lower than the efficiency measured later with more stable temperatures. In another case, with a collector system of greater thermal mass, a similar slow drift in input temperature produced an efficiency measurement 15 percentage points lower than the true value.

If the input temperature drift is towards lower temperatures, errors of similar magnitude result, but the measured efficiency will be greater than the value obtained under stable conditions.

The same problem as outlined above for an efficiency measurement also occurs during thermal loss measurements. The error in thermal loss from unstable temperatures is larger than the efficiency error because the receiver delta temperature during a loss test is usually much less than during an efficiency measurement.

The requirement for $0.1^{\circ}C$ stability in measured temperatures for a usable data point is empirically based. It appears to produce valid data, and is also about as good as the fluid loop and collector system can attain in the outdoor test environment.

TEST RESULTS: The performance of the McDonnell Douglas collector at specific operating temperatures is graphically portrayed in the following seven figures (6-13). Each set of data (one for solar radiation, one for efficiency) is a result of a data measurement cycle that is recurring at ≈40-second intervals. The flow-rate and input/output temperatures shown in the captions in each plot are those that occurred at solar noon. In general, the input temperatures were held constant throughout the day, and the output temperatures varied depending on the solar input. Flow-rate variations that are significant are given on the figures.

Figure 6 depicts the results of an all-day run at 149°C input temperature. This test was distrubed by a fluctuating solar input, but the results are interesting. Other tests had indicated that the collector efficiency was nearly the same for solar inputs above about 800 W/m^2 (see Figures 9 and 10). Figure 6 tends to show the same thing. Most of the scatter in the efficiency plot is caused by the thermal mass of the system. The temperatures which are measured are the result of the solar input over a period of many minutes and do not follow the fast fluctuations in solar radiation.

Figure 7 again demonstrates the drastic effect that a momentary interruption in solar input can have on an efficiency measurement. After a 3 minute solar interruption by a small cloud at about 1015 the efficiency curve does not return to stable conditions for at least 5 times this time span. Figure 7 also shows that there is an efficiency change with different fluid flow-rates. This effect was confirmed on several other tests.

The plots in Figure 8 depict the exceptional stability of efficiency measurements that can be taken with an uninterrupted solar input, stable temperatures and constant flow-rate. The varying efficiency levels resulted from the changes in flow-rate that are noted on the plot. The curves are not shown earlier than about 1030 because of the time required to heat the system to the desired operating temperature. The curves terminate at about 1420 when the collector was defocused to begin thermal loss tests.

The curves in Figure 9 begin even later than those in Figure 8 because of the extra heating time required to reach the higher operating temperature. Note the clear steps in the efficiency curve in Figure 9 as the fluid flow-rate was increased.

The curves in Figure 10 are the result of an all-day run at about 250°C. Heating of the system was started well before sunrise, but the required input temperature was not achieved until just after 1000. The jump in the efficiency curve from 38% at 1004 to 43% at 1028 is entirely a result of stabilizing the fluid temperatures so that the thermal mass of the system did not cause errors in the efficiency measurements. Prior to 1000, the input and output temperatures were increasing at about 0.7°C per minute. From 1028 to 1042, the desired stability of 0.1°C was achieved and flow-rates were constant to within 0.1 L/min. The perturbation visible in the efficiency plot in Figure 10 at about 0845 was caused by washing the collector lenses; a "spike" at 1045 resulted from a momentary change of flow-rate, and a break at 1315 resulted when the platinum resistance thermometers were recalibrated.

Figure 11 presents the results of a run at 298°C. The 2% step in the efficiency curve beginning at 1205 is the result of stopping a heating rate of about 0.2°C per minute, and stabilizing the input temperature at 300°C. The remaining steps in the efficiency curve are the result of the flow-rate changes that are noted on the figure.

Figure 12 presents a summary plot of the results of the series of efficiency measurements. Table 1 contains the data from which the plot was made. At the highest flow-rates the efficiency decreased from about 58% near 100°C to about 47% near

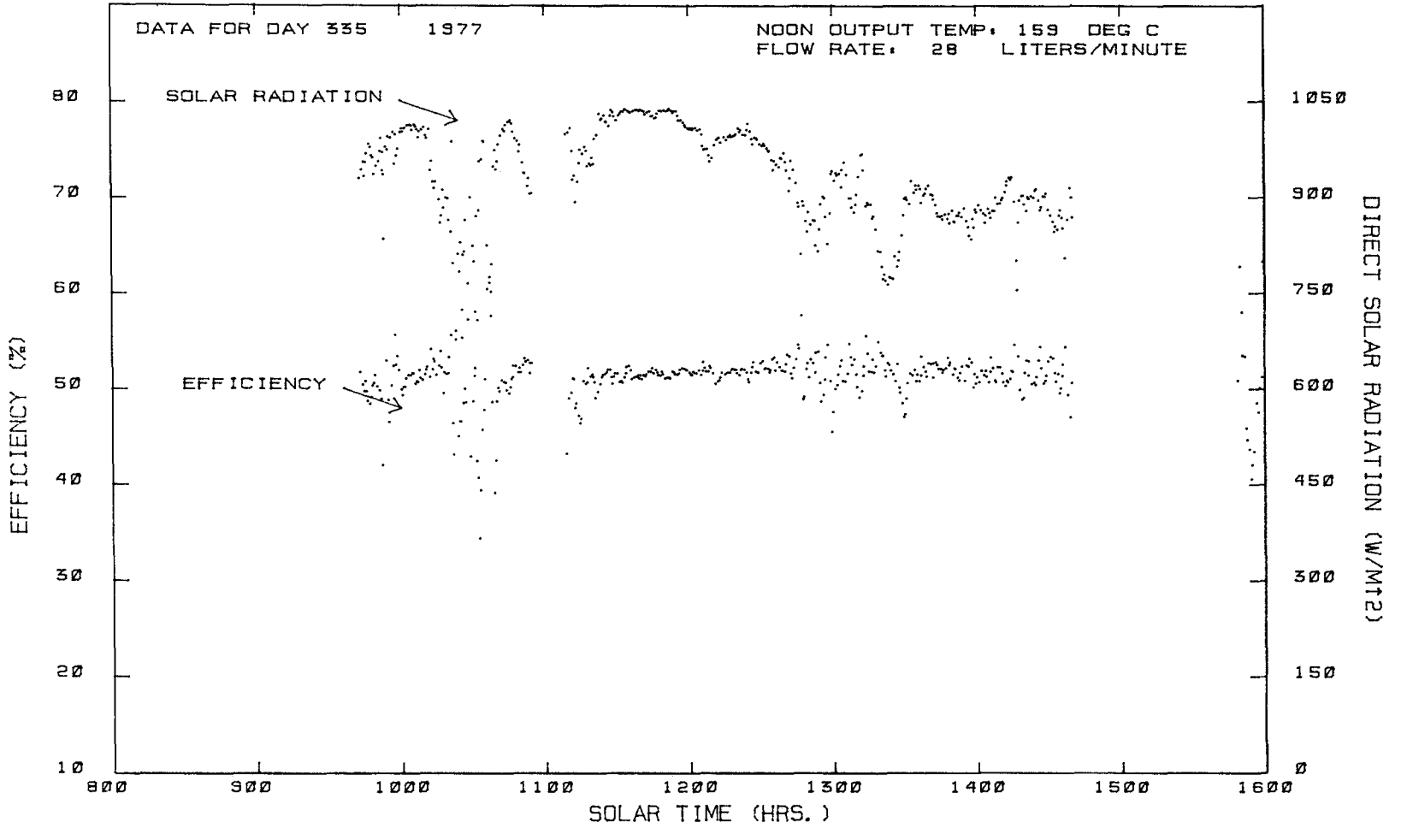

FIGURE 6 MCDONNELL DOUGLAS EFFICIENCY EVALUATION AT 149 DEG C INPUT

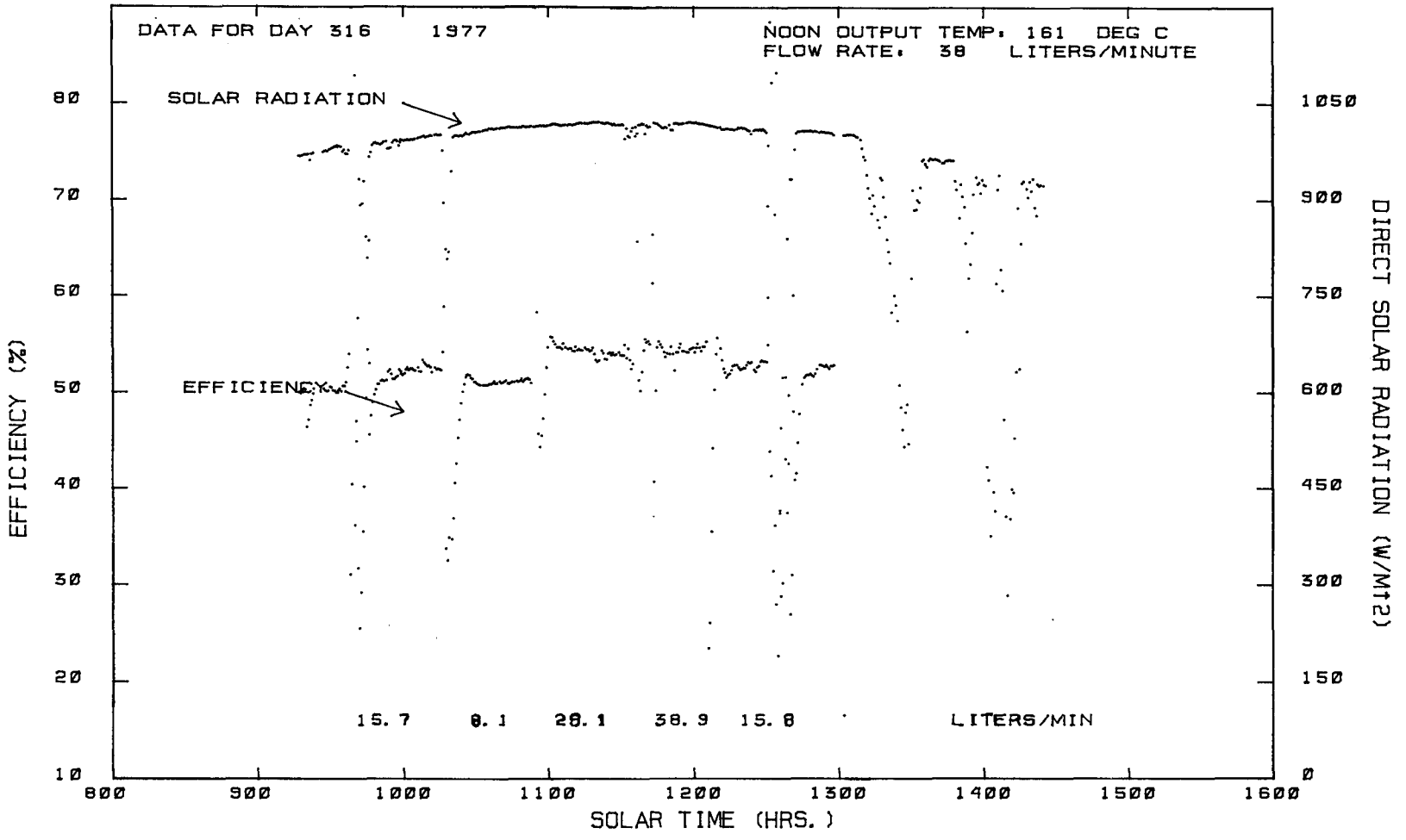

FIGURE 7 MCDONNELL DOUGLAS EFFICIENCY EVALUATION AT 154 DEG C INPUT

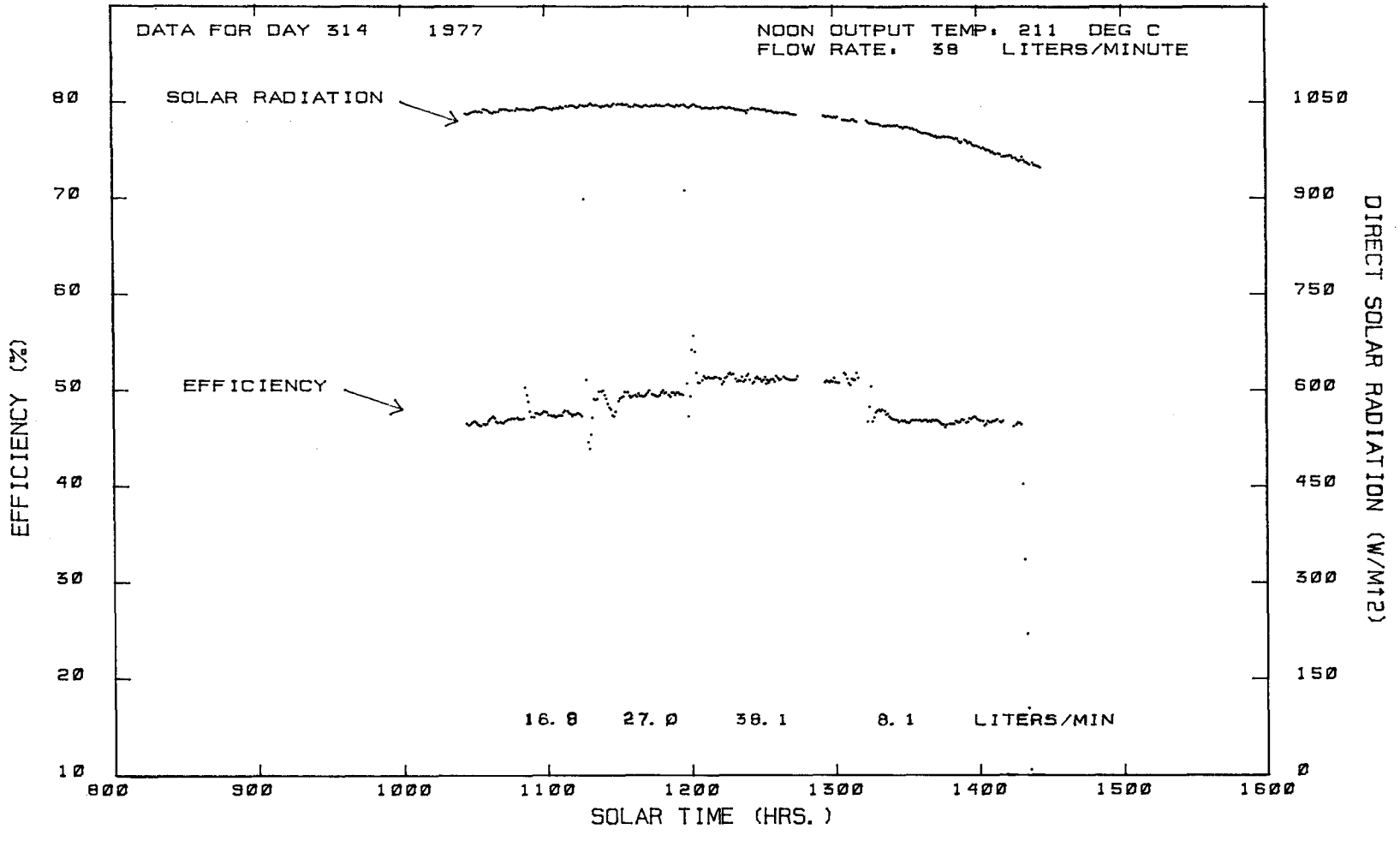

FIGURE 8 MCDONNELL DOUGLAS EFFICIENCY EVALUATION AT 204 DEG C INPUT

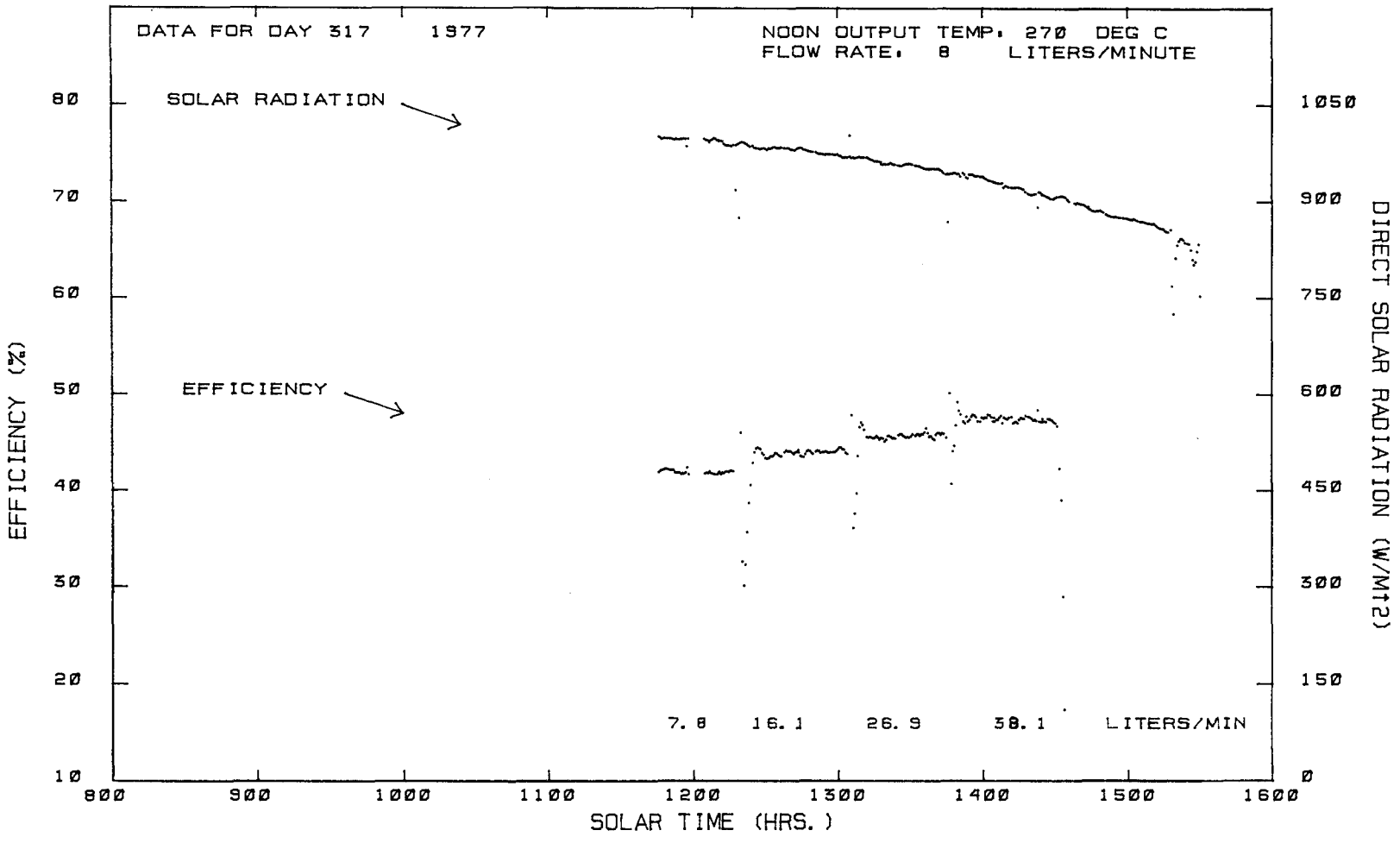

FIGURE 9 MCDONNELL DOUGLAS EFFICIENCY EVALUATION AT 245 DEG C INPUT

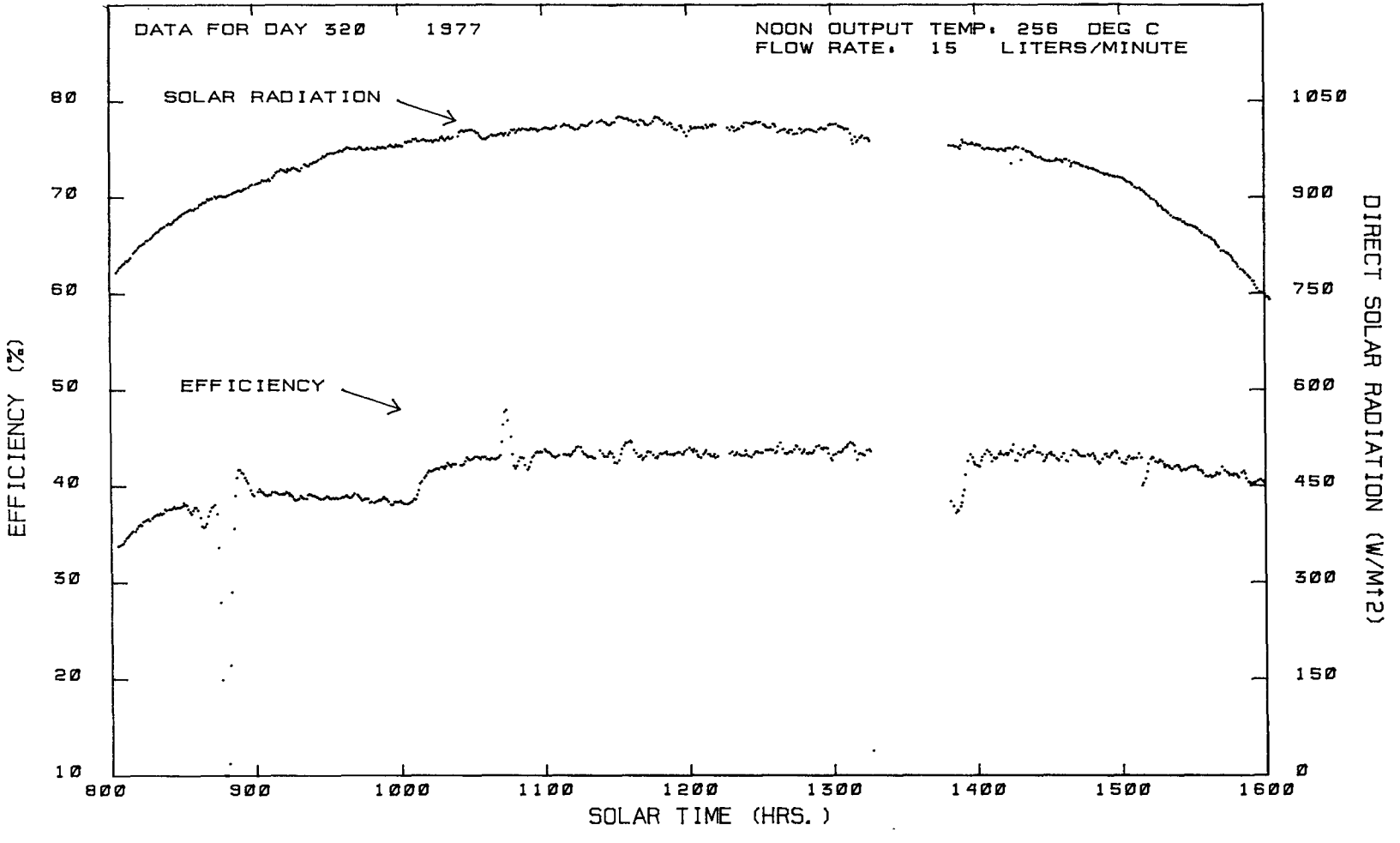

FIGURE 10 MCDONNELL DOUGLAS EFFICIENCY EVALUATION AT 243 DEG C INPUT

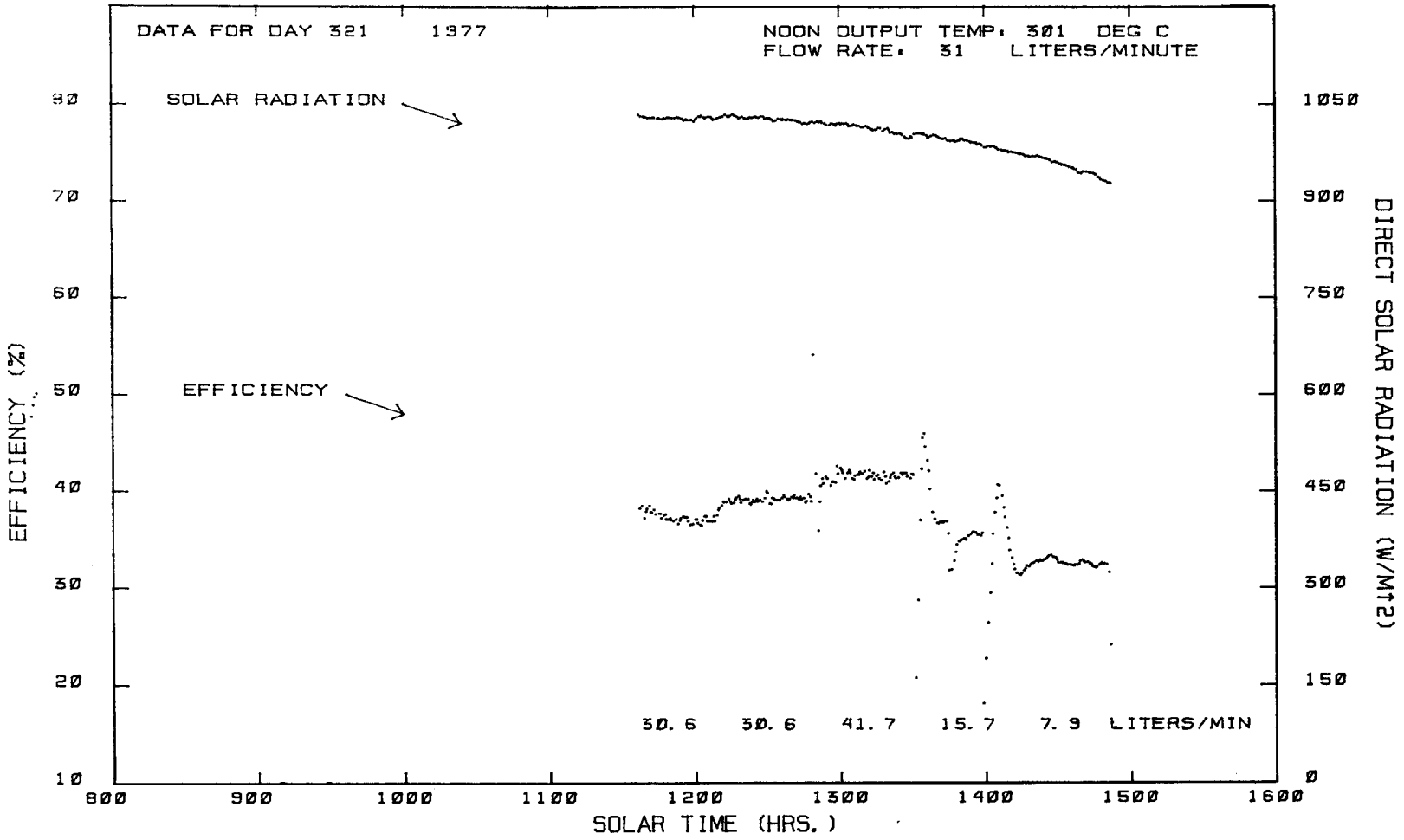

FIGURE 11 MCDONNELL DOUGLAS EFFICIENCY EVALUATION AT 298 DEG C INPUT

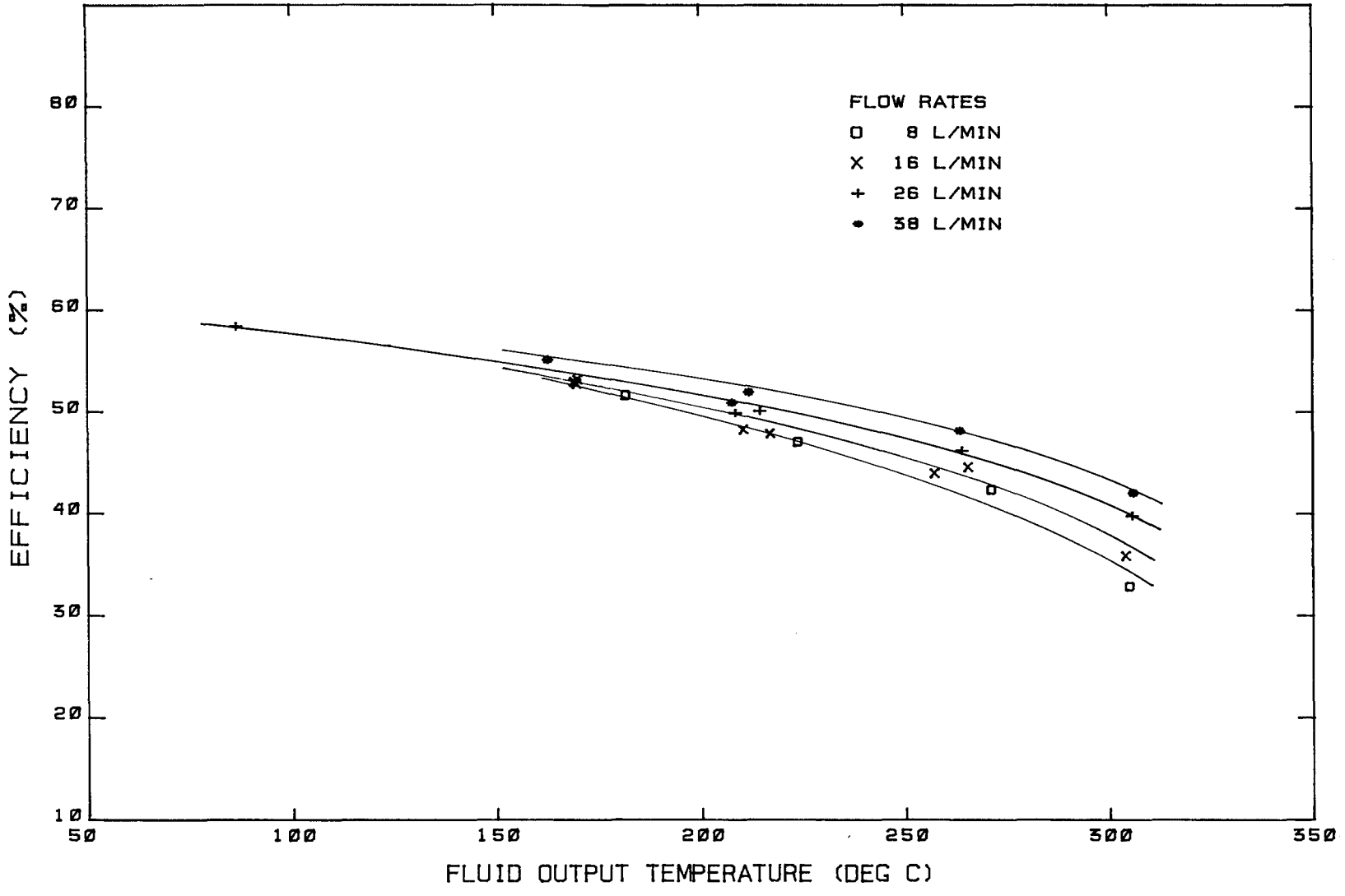

FIGURE 12 MCDONNELL DOUGLAS EFFICIENCY VS OUTPUT TEMP.

300°C. Efficiencies were several percent lower at the lower flow-rates, possibly due to the onset of laminar fluid flow within the absorber tubes.

Table 1. Efficiency of McDonnell Douglas Solar Collector.

Test Date	Insolation (W/m^2)	Temperature Out (°C)	Receiver Δ Temperature (°C)	Flow-Rate (L/min)	Efficiency (%)
11/10/77	1044	216.2	14.3	16.8	47.5
11/10/77	1047	213.3	9.3	27.1	49.6
11/10/77	1024	210.4	6.7	38.1	51.3
11/10/77	974	222.9	27.1	8.1	46.7
11/12/77	999	168.2	16.6	16.0	52.6
11/12/77	1014	180.8	32.0	8.1	51.3
11/12/77	1021	161.2	7.4	38.3	54.5
11/12/77	1006	169.1	17.0	16.0	52.8
11/13/77	990	270.3	24.9	7.8	42.0
11/13/77	971	264.6	12.5	16.0	44.2
11/13/77	950	262.6	7.5	26.9	45.7
11/13/77	935	262.0	5.4	38.1	47.5
11/15/77	981	168.9	17.7	14.6	52.4
11/16/77	1007	256.3	13.4	15.4	43.6
11/17/77	1026	304.3	3.4	30.7	39.3
11/17/77	1009	304.4	2.3	41.6	41.4
11/17/77	991	303.2	6.5	15.7	35.5
11/17/77	948	304.0	12.2	7.9	32.5
11/23/77	973	209.6	9.2	17.2	47.9
11/23/77	938	207.3	5.1	28.7	49.9
11/23/77	918	206.3	3.6	37.8	50.3
12/02/77	988	85.2	11.0	28.9	57.9

Figure 13 is based on the same efficiency data, but the efficiency is plotted against ΔT/I (the average fluid temperature minus the ambient temperature, divided by the solar radiation input). Testing of this collector was accomplished over a somewhat greater range of solar radiation levels than is the normal practice at the CMTF; the result is increased data scatter in Figure 13.

Figure 14 presents the data from the thermal loss tests that were conducted on the McDonnell Douglas solar collector. In Figure 14, the right ordinate is the measured thermal loss in watts, the left ordinate shows the thermal loss per square meter of lens aperture area, and the loss per linear meter of heated pipe within the collector box.

The curve shown in Figure 14 is a least-squares fit to the data points shown. The equation for the curve is:

$$L = -5.7675 + 4.0869\ T + 0.021105\ T^2$$

where

L = thermal loss (watts)

T = temperature above ambient (°C)

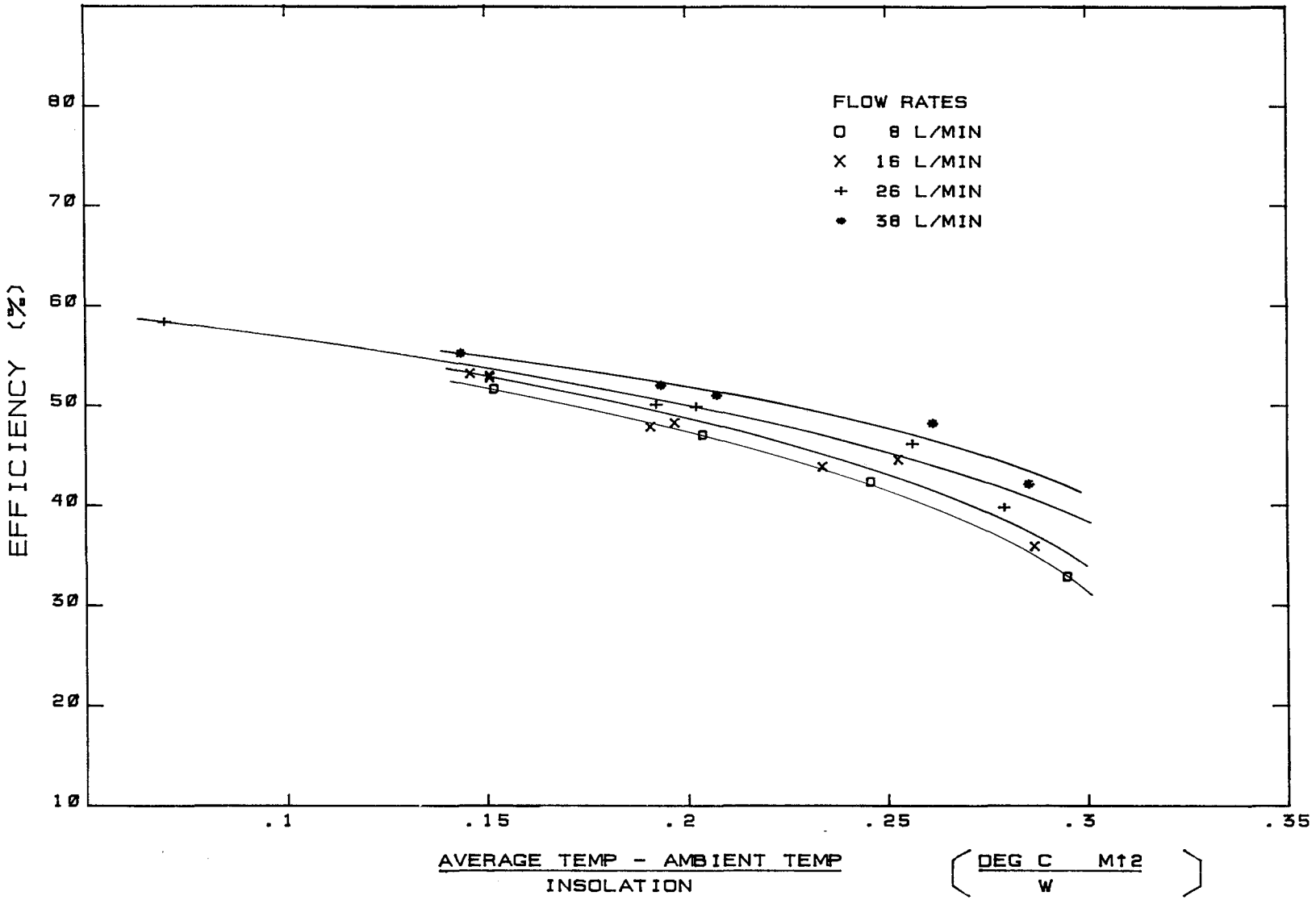

FIGURE 13 MCDONNELL DOUGLAS EFFICIENCY VS DELTA T/I

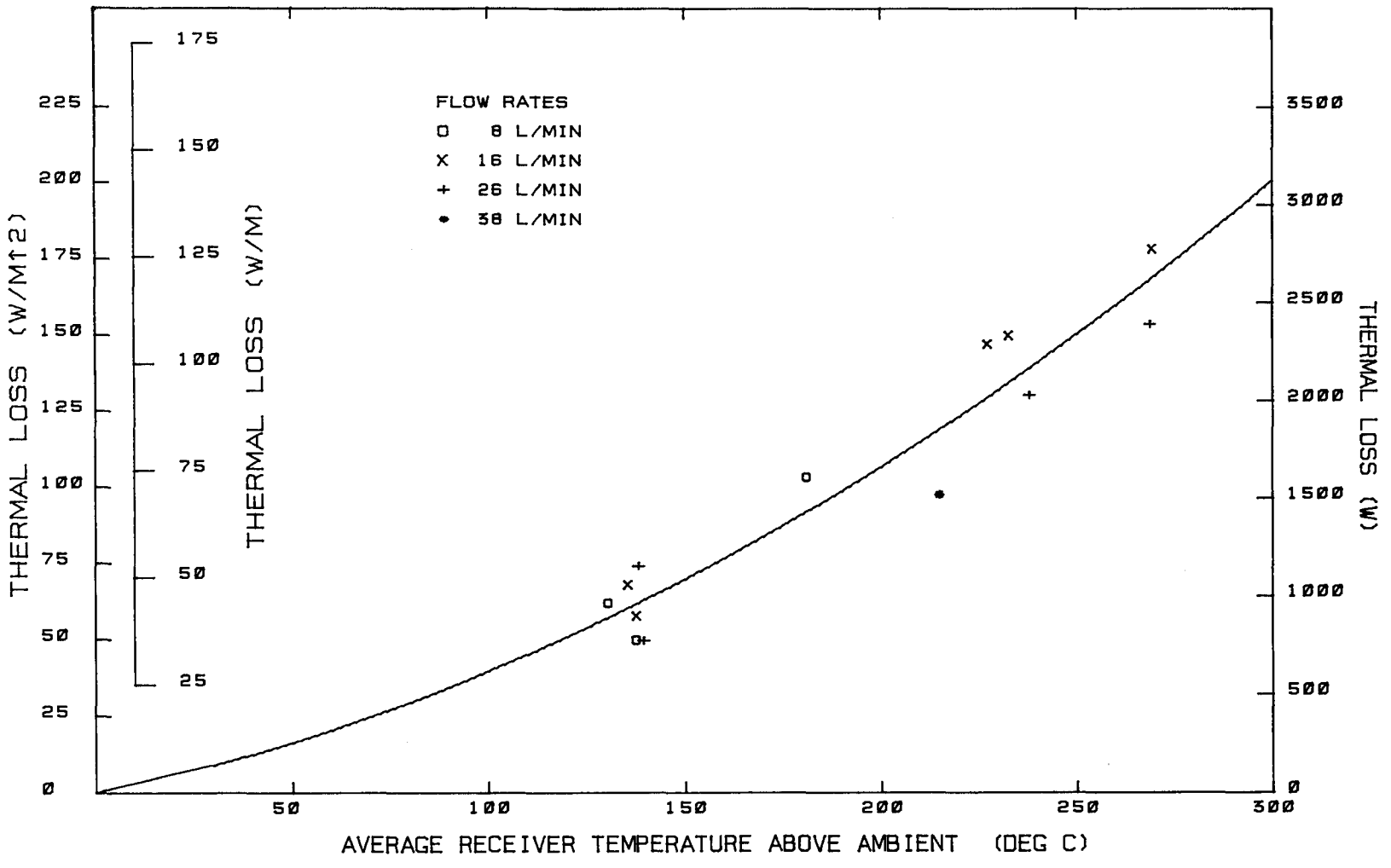

FIGURE 14 MCDONNELL DOUGLAS RECEIVER THERMAL LOSS

Table 2 contains details of each individual point. No dependence of thermal loss on flow-rate was found. Because of the fully enclosed design, little wind effect would be expected and no attempt was made to characterize wind effects. Several points were measured with little or no solar radiation present and these points show greater thermal losses (which was expected), but are not representative of the losses during normal operation.

Table 2. McDonnell Douglas Thermal Losses.

Test Date	Input Temperature (°C)	Receiver Temperature (°C)	Flow (L/min)	Loss (kJ/hr)	Wind (m/sec)	Ambient Temperature (°C)	Solar Radiation (W/m^2)
11/10/77	194.3	6.3	8.1	5709	2.2	11.1	916
11/12/77	152.1	1.8	15.7	3157	0.9	14.6	--
11/12/77	153.5	0.8	31.4	2689	1.8	15.0	--
11/13/77	253.9	2.1	29.8	7207	0.9	16.3	877
11/13/77	250.2	4.8	14.9	8319	1.3	16.1	794
10/14/77	154.3	3.3	7.6	2718	2.2	16.2	779
10/17/77	288.5	4.9	16.7	9917	0.9	17.8	828
10/17/77	286.8	2.9	29.8	8510	2.7	18.0	746
10/18/77	145.1	3.7	8.4	3398	2.2	13.8	4.2
10/18/77	149.7	2.2	15.5	3729	2.2	14.1	1.5
10/18/77	151.2	1.2	30.3	4053	2.7	13.9	1.7
10/22/77	242.0	4.2	16.0	8161	2.2	13.7	42.1
10/22/77	229.2	1.7	38.8	5328	0.9	14.9	378

The sun-tracking sensor was mounted at the bottom of the collector box structure. This location was only about one m above the surface during early morning and late afternoon operation. As a result of the bottom-mount location, the sensor was easily mislead by shadows and reflections during these periods. A location near the top of the structure would eliminate most of these distractions although the top-mount would be more inconvenient for adjustments or servicing.

SUMMARY OF RESULTS AND CONCLUSIONS: The McDonnell Douglas Linear Fresnel Lens Rotating Array Solar Collector demonstrated an efficiency of about 58% near 100°C, decreasing to about 47% near 300°C output temperature. Efficiencies were several percent lower at low fluid flow-rates, probably due to the onset of laminar flow within the receiver.

The measured efficiencies were lower than predicted. Detailed optical measurements are not presently available to determine the causes of the lower efficiency. Possible factors include lower than expected light transmission through the acrylic Fresnel lens, inaccurate focus of the light on the absorber, and lower than normal absorptivity of the absorber surface. The collector has been returned to McDonnell Douglas for further testing. Optical measurements of the lens characteristics, accuracy of the focal line and absorptivity and emmitance of the absorber surface may produce a more detailed picture of the light losses.

Even with a peak efficiency slightly lower than some other collectors, this collector design can produce a large energy recovery on an all-day basis

because of its two-axis tracking capability. The energy represented by the all-day test shown in Figure 11 is about 11.2 MJ/m^2. A single-axis parabolic trough collector would have to have a peak noon efficiency about 12% greater than the McDonnell Douglas module to recover the same energy in a similar eight-hour day.

REFERENCES

1. Solar Total Energy Program Plan, SAND76-0167, (revised) August 1976, Sandia Laboratories, Albuquerque, New Mexico.

2. Therminol 66, Technical Data Sheet, IC/FF-35, Monsanto Company.

3. Harrison, T.; Dworzak, W.; and Folkner, C., Solar Collector Module Test Facility, Instrumentation Fluid Loop Number One, SAND76-0425, January 1977, Sandia Laboratories, Albuquerque, New Mexico.

DISTRIBUTION:
TID-4500-R66, UC62 (316)

Aerospace Corporation
101 Continental Blvd.
El Segundo, CA 90245
Attn: Elliott L. Katz

Acurex Aerotherm
485 Clyde Avenue
Mountain View, CA 94042
Attn: G. J. Neuner

Solar Total Energy Program
American Technological Univ.
P.O. Box 1416
Killeen, TX 76541
Attn: B. L. Hale

Argonne National Laboratory (3)
9700 South Cass Avenue
Argonne, IL 60439
Attn: R. G. Matlock
W. W. Schertz
Roland Winston

Atlantic Richfield Co.
515 South Flower Street
Los Angeles, CA 90071
Attn: H. R. Blieden

Barber Nichols Engineering
6325 W. 55th Avenue
Arvada, CO 80002
Attn: R. G. Olander

Battelle Memorial Institute
Pacific Northwest Laboratory
P.O. Box 999
Richland, WA 99352
Attn: K. Drumheller

Brookhaven National Laboratory
Associated Universities, Inc.
Upton, LI, NY 11973
Attn: J. Blewett

Congressional Research Service
Library of Congress
Washington, DC 20540
Attn: H. Bullis

Del Manufacturing Co.
905 Monterey Pass Road
Monterey Park, CA 91754
Attn: M. M. Delgado

Desert Research Institute
Energy Systems Laboratory
1500 Buchanan Blvd.
Boulder City, NV 89005
Attn: Jerry O. Bradley

DSET
Black Canyon Stage
P. O. Box 185
Phoenix, AZ 85029
Attn: Gene A. Zerlaut

Honorable Pete V. Domenici
Room 405
Russell Senate Office Bldg.
Washington, DC 20510

Edison Electric Institute
90 Park Avenue
New York, NY 10016
Attn: L. O. Elsaesser,
Director of Research

Energy Institute
1700 Las Lomas
Albuquerque, NM 87131
Attn: T. T. Shishman

EPRI
3412 Hillview Avenue
Palo Alto, CA 94303
Attn: J. E. Bigger

General Atomic
P. O. Box 81608
San Diego, CA 92138
Attn: Alan Schwartz

General Electirc Company
Valley Forge Space Center
Valley Forge, PA 19087
Attn: Walt Pijawka

General Electric Co.
P.O. Box 8661
Philadelphia, PA 19101
Attn: A. J. Poche

Georgia Institute of Technology
School of Mechanical Engineering
Atlanta, GA 30332
Attn: S. Peter Kezios,
President
American Society of
Mechanical Engineers

Georgia Institute of Technology
Atlanta, GA 30332
Attn: J. D. Walton

Georgia Power Company
Atlanta, GA 30302
Attn: Mr. Walter Hensley
Vice President
Economics Services

Gruman Corporation
4175 Veterans Memorial Highway
Ronkonkoma, NY 11779
Attn: Ed Diamond

Hexcel
11711 Dublin Blvd.
Dublin, CA 94566
Attn: George P. Branch

Industrial Energy Control Corp.
118 Broadway
Hillsdale, NJ 07675
Attn: Peter Groome

Jet Propulsion Laboratory
4800 Oak Grove Drive
Pasadena, CA 91103
Attn: V. C. Truscello

Kingston Industries
205 Lexington Avenue
New York, NY 10016
Attn: Ken Brandt

DISTRIBUTION (Cont)
Lawrence Berkley Laboratory
University of California
Berkley, CA 94720
Attn: Mike Wallig

Lawrence Livermore Laboratory
University of California
P.O. Box 808
Livermore, CA 94500
Attn: W. C. Dickinson

Los Alamos Scientific Lab. (3)
Los Alamos, NM 87545
Attn: J. D. Balcomb
C. D. Bankston
D. P. Grimmer

Honrable Manuel Lujan
1324 Longworth Building
Washington, DC 20515

Mann-Russell Electronics, Inc.
1401 Thorne Roade
Tacoma, WA 98421
Attn: G. F. Russell

Martin Marietta Aerospace
P.O. Box 179
Denver, CO 80201
Attn: R. C. Rozycki

McDonnell Douglas Astronautics Co.
5301 Bolsa Avenue
Huntington Beach, CA 92647
Attn: Don Steinmeyer

NASA-Lewis Research Center
Cleveland, OH 44135
Attn: R. Hyland

New Mexico State University
Solar Energy Department
Las Cruces, NM 88001

Oak Ridge Associated Universities
P.O. Box 117
Oak Ridge, TN 37830
Attn: A. Roy

Oak Ridge National Laboratory (4)
P.O. Box Y
Oak Ridge, TN 37830
Attn: J. R. Blevins
C. V. Chester
J. Johnson
S. I. Kaplan

Office of Technology Assessment
U. S. Congress
Washington, DC 20510
Attn: Dr. Henry Kelly

Omnium G (2)
1815 Orangethorpe Park
Anaheim, CA 92801
Attn: Ron Derby
S. P. Lazzara

PRC Energy Analysis Company
7600 Old Springhouse Road
McLean, VA 22102
Attn: K. T. Cherian

Rocket Research Company
York Center
Redmond, WA 98052
Attn: R. J. Stryer

Honorable Harold Runnels
1535 Longworth Building
Washington, DC 20515

Honorable Harrison H. Schmitt
Room 1251
Dirksen Senate Office Bldg.
Washington, DC 20510

Scientific Atlanta, Inc.
3845 Pleasantdale Road
Atlanta, Georgia 30340
Attn: Andrew L. Blackshaw

Sensor Technology, Inc.
21012 Lassen Street
Chatsworth, CA 91311
Attn: Irwin Rubin

Solar Energy Research Institute (7)
1536 Cole Blvd.
Golden, CO 80401
Attn: C. J. Bishop
Ken Brown
B. L. Butler
Frank Kreith
Charles Grosskreutz
B. P. Gupta
A. Rabl

Solar Energy Technology
Rocketdyne Division
6633 Canoga Avenue
Canoga Park, CA 91304
Attn: J. M. Friefeld

Solar Kinetics Inc.
P.O. Box 10764
Dallas, TX 75207
Attn: Gus Hutchison

Southwest Research Institute
P.O. Box 28510
San Antonio, TX 78284
Attn: Danny M. Deffenbaugh

Stanford Research Institute
Menlo Park, CA 94025
Attn: Arthur J. Slemmons

Stone & Webster
Box 5406
Denver, CO 80217
Attn: V. O. Staub

Sun Gas Company
Suite 800, 2 No. Pk. E
Dallas, TX 75231
Attn: R. C. Clark

Sundstrand Electric Power
4747 Harrison Avenue
Rockford, IL 61101
Attn: A. W. Adam

Sunsearch, Inc.
669 Boston Post Road
Guilford, CT 06437
Attn: E. M. Barber, Jr.

DISTRIBUTION (Cont)
Suntec System Inc.
21405 Hamburg Avenue
Lakeville, MN 55044
Attn: J. H. Davison

Swedlow, Inc.
12122 Western Avenue
Garden Grove, CA 92645
Attn: E. Nixon

TEAM Inc.
8136 Ola Keene Mill Road
Springfield, VA 22152

U.S. Department of Energy (2)
Agricultural & Industrial
Process Heat
Conservation & Solar Application
Washington, DC 20545
Attn: W. W. Auer
J. Dollard

U. S. Department of Energy (3)
Albuquerque Operations Office
P. O. Box 5400
Albuquerque, NM 87185
Attn: D. K. Nowlin
G. Pappas
J. R. Roder

U.S. Department of Energy
Division of Energy Storage Systems
Washington, DC 20545
Attn: C. J. Swet

U. S. Department of Energy (9)
Division of Central Solar Technology
Washington, DC 20545
Attn: R. H. Annan
G. W. Braun
H. Coleman
M. U. Gutstein
G. M. Kaplan
Lou Melamed
J. E. Rannels
M. E. Resner
J. Weisiger

U.S. Department of Energy
Los Angeles Operations Office
350 S. Figueroa Street
Suite 285
Los Angles, CA 90071
Attn: Fred A. Glaski

U.S. Department of Energy
San Francisco Operations Office
1333 Broadway, Wells Fargo Bldg.
Oakland, CA 94612
Attn: Jack Blasy

University of Delaware
Institute of Energy Conversion
Newark, DE 19711
Attn: K. W. Boer

University of New Mexico (2)
Department of Mechanical Eng.
Albuquerque, NM 87113
Attn: W. A. Cross
M. W. Wilden

Watt Engineering Ltd.
RR1 Box 183 1/2
Cedaredge, CO 81413
Attn: A. D. Watt

Western Control System
13640 Silver Lake Drive
Poway, CA 92064
Attn: L. P. Cappiello

Westinghouse Electric Corp.
P.O. Box 10864
Pittsburgh, PA 15236
Attn: J. Buggy

1100 C. D. Broyles
1500 W. A. Gardner
1520 T. L. Pace
1530 W. E. Caldes
1540 R. L. Brin
1550 F. W. Neilson
1552 O. N. Burchett
2300 J. C. King
2320 K. L. Gillespie
2323 C. M. Gabriel
2324 L. W. Schulz
2326 G. M. Heck
3161 J. E. Mitchell
3700 J. C. Strassell
4000 A. Narath
4531 J. H. Renken
4700 J. H. Scott
4710 G. E. Brandvold
4713 B. W. Marshall
4714 R. P. Stromberg
4715 R. H. Braasch
4719 D. G. Schueler
4720 V. L. Dugan
4721 J. V. Otts (250)
4722 J. F. Banas
4723 W. P. Schimmel
4725 J. A. Leonard
4730 H. M. Stoller
5450 R. C. Wayne
5512 H. C. Hardee
5520 T. B. Lane
5524 R. T. Othmer
5600 D. B. Shuster
5630 R. C. Maydew
5834 D. M. Mattox
Attn: 5831 N. J. Magnani
5840 H. J. Saxton
Attn: 5810 R. G. Kepler
5820 R. L. Schwoebel
5830 M. J. Davis
5844 F. P. Gerstle
Attn: 5842 J. N. Sweet
5846 E. K. Beauchamp
8100 L. Gutierrez
8451 W. G. Wilson
8452 A. C. Skinrood
8453 J. D. Gilson
8266 E. A. Aas
8470 C. S. Selvage
9572 L. G. Rainhart
9700 R. W. Hunnicutt
Attn: H. H. Pastorius, 9740
3141 T. L. Werner (5)
3151 W. L. Garner (3)
For DOE/TIC
(Unlimited Release